Adjuvant selection regulates gut migration and phenotypic diversity of antigen-specific CD4$^+$ T cells following parenteral immunization

DR Frederick[1], JA Goggins[1], LM Sabbagh[1], LC Freytag[1], JD Clements[1] and JB McLachlan[1]

Infectious diarrheal diseases are the second leading cause of death in children under 5 years, making vaccines against these diseases a high priority. It is known that certain vaccine adjuvants, chiefly bacterial ADP-ribosylating enterotoxins, can induce mucosal antibodies when delivered parenterally. Based on this, we reasoned vaccine-specific mucosal cellular immunity could be induced via parenteral immunization with these adjuvants. Here, we show that, in contrast to the Toll-like receptor-9 agonist CpG, intradermal immunization with non-toxic double-mutant heat-labile toxin (dmLT) from enterotoxigenic *Escherichia coli* drove endogenous, antigen-specific CD4$^+$ T cells to expand and upregulate the gut-homing integrin α4β7. This was followed by T-cell migration into gut-draining lymph nodes and both small and large intestines. We also found that dmLT produces a balanced T-helper 1 and 17 (Th1 and Th17) response, whereas T cells from CpG immunized mice were predominantly Th1. Immunization with dmLT preferentially engaged CD103$^+$ dendritic cells (DCs) compared with CpG, and mice deficient in CD103$^+$ DCs were unable to fully license antigen-specific T-cell migration to the intestinal mucosae following parenteral immunization. This work has the potential to redirect the design of existing and next generation vaccines to elicit pathogen-specific immunity in the intestinal tract with non-mucosal immunization.

INTRODUCTION

Vaccines are one of the most successful medical interventions ever devised. Despite these successes, more children die every day from infectious diarrheal diseases than from malaria, HIV, and measles combined.[1] Although many vaccines are excellent at inducing systemic humoral immunity, vaccines that elicit cellular immunity, specifically in the mucosa, are rare. One way to circumvent this issue would be to deliver vaccines directly to the mucosa, and although some vaccines are delivered mucosally (predominantly orally) and are efficacious in developed countries, they often fail to protect children in developing countries, a phenomenon known as environmental enteropathy. An example of this is the live oral polio vaccine, which requires many more immunizations to achieve equivalent protective levels of immunity in children in developing countries compared with those where health care is more accessible and modernized.[2] Multiple factors appear to be responsible for this; however, inadequate polio vaccine colonization of the intestinal mucosae due to ongoing diarrheal disease appears to play a meaningful role.[3,4] This creates something of a paradox in that the very diseases requiring new vaccines may prevent oral immunization from being effective.

Avoiding the deficiencies of mucosally delivered vaccines would be an important step in combatting enteric diseases in developing countries. One attractive possibility would be to deliver vaccines parenterally and use the vaccine formulation itself to dictate the nature and location of the immune response. Most previous studies were directed at assessing humoral immunity to parenterally delivered vaccines.[5–7] How non-mucosal immunization affects antigen-specific T-cell responses at the intestinal mucosae is poorly understood. It is also known that the correct parenteral route must be combined with an appropriate adjuvant to achieve mucosal immunity, yet the list of adjuvants that can promote mucosal responses is short, but includes bacterial ADP-ribosylating enterotoxins such as cholera toxin.[7–9] In this study, we sought to determine

[1]Department of Microbiology and Immunology, Tulane University School of Medicine, New Orleans, Louisiana, USA. Correspondence: JB McLachlan (jmclachl@tulane.edu)

Received 22 October 2016; accepted 28 June 2017; published online 9 August 2017. doi:10.1038/mi.2017.70

how the choice of adjuvant, when delivered parenterally, could affect intestinal homing and phenotype of endogenous, antigen-specific $CD4^+$ T cells and furthermore, what antigen presenting cells might dictate this type of response.

We used major histocompatibility complex class II tetramers to detect endogenous $CD4^+$ T cells specific for a model antigen. We found that, when injected intradermally, the adjuvant double-mutant heat-labile toxin (dmLT), derived from enterotoxigenic *E. coli*, specifically upregulated the intestinal homing integrin α4β7 on antigen-specific T cells. This was in contrast to the well-studied Toll-like receptor-9 agonist adjuvant CpG, which did not increase α4β7 expression to the same degree. Moreover, dmLT drove preferential migration of these antigen-specific T cells into both the small and large intestine. Expectedly, CpG induced an almost exclusive T-helper 1 (Th1) T-cell phenotype; however, dmLT produced T cells displaying a more balanced Th1/Th17 phenotype. In addition, dmLT preferentially engaged $CD103^+$ dendritic cells (DCs) compared with CpG. This is notable as CD103 expression on DCs is linked to mucosal homing on primed $CD4^+$ T cells.[10–12] Lastly, gut homing phenotypes appeared to be independent of parenteral route, as intramuscular injection induced similar outcomes. These results demonstrate the importance of the choice of adjuvant in dictating the cellular immune responses in the intestine when vaccines are delivered parenterally and have the potential to change how future vaccines are designed.

RESULTS

dmLT sustains a potent, endogenous antigen-specific $CD4^+$ T-cell response

We first attempted to dissect the overall kinetics of the endogenous, antigen-specific $CD4^+$ T-cell response to immunization with dmLT compared with the well-described Toll-like receptor-9 agonist CpG. Mice were injected intradermally in the ear with either dmLT or CpG, plus a protein antigen containing the well-characterized major histocompatibility complex class II ($I\text{-}A^b$) $CD4^+$ T-cell epitope $2W1S^{13–16}$ fused to green fluorescent protein (hereafter 2W1S-GFP). After 4, 9, 14, 28, and 56 days, we used 2W1S:$I\text{-}A^b$ tetramers to assess the number of 2W1S-specific T cells in the ear-draining cervical lymph nodes (CLNs) and spleen. Throughout, the 2W1S-specific $CD4^+$ T-cell population showed dmLT induced a greater expansion compared with the CpG immunized group across all time points (**Supplementary Figure S1A** online). Within the draining CLN, dmLT and CpG immunization induced peak expansion of 2W1S-specific T cells 9 days after intradermal immunization, with dmLT inducing greater overall numbers of Ag-specific $CD4^+$ T cells. By 14 days, antigen-specific $CD4^+$ T-cell responses began to decline in the CLN in both groups, but there remained a higher number migrating to the spleen in the dmLT-immunized mice, suggesting a greater overall peak response for 2W1S-specific $CD4^+$ T cells in the dmLT immunized group. During the memory phase (days 28–56), systemic responses in the spleen were reduced compared with day 14, whereas the CLN response appeared to plateau. By day 56, the number of 2W1S-specific T cells were maintained in the spleen and remained higher in dmLT-immunized mice, potentially highlighting the capacity for dmLT to induce a more sustained memory response. These results demonstrated that dmLT was the superior adjuvant compared with CpG, at least for expanding and maintaining endogenous, antigen-specific $CD4^+$ T cells in systemic lymphoid tissues.

dmLT preferentially induces α4β7 integrin on antigen-specific $CD4^+$ T cells and induces mucosal homing

Although the previous results showed that dmLT excelled at inducing antigen-specific $CD4^+$ T-cell responses in local draining lymph nodes, it was unclear whether these responses were confined to this site. It is known that ADP-ribosylating adjuvants such as dmLT or cholera toxin induce intestinal humoral immunity,[7,17,18] so we investigated whether they could induce antigen-specific T-cell migration to the gut when administered parenterally. Initially, we assessed the absolute number of 2W1S-specific $CD4^+$ T cells and demonstrated that dmLT was a more potent adjuvant compared with CpG (**Supplementary Figure S1A**). We next examined whether dmLT preferentially upregulated the intestinal homing integrin α4β7 in comparison to CpG. From day 4 to day 28, dmLT induced a greater total number of Ag-specific $CD4^+$ T cells migrating systemically (in spleen) that expressed α4β7 (**Supplementary Figure S1B**). This observation regarding $\alpha4\beta7^+$ $CD4^+$ T-cell numbers could simply have been a function of the greater total magnitude of dmLT-induced 2W1S-specific T cells. To examine this, mice immunized with either dmLT or CpG plus 2W1S-GFP were assayed for lymph node responses using 2W1S:$I\text{-}A^b$ tetramer enrichment and the percentage of 2W1S-specific T cells and α4β7 expression in this 2W1S-specific fraction was determined.[19] Local responses in the skin-draining CLN were much higher after dmLT injection at day 4, having nearly three times the percentage of $CD4^+$ T cells specific for 2W1S compared with CpG (**Figure 1a** and **b**). Importantly, the proportion of 2W1S-specific cells expressing α4β7 was also significantly higher in the case of dmLT (**Figure 2a** and **b**). At the peak of the response (day 9) the 2W1S-specific responses remained higher in the dmLT immunized group in the CLN, and more 2W1S-specific T cells were expressing more α4β7 when dmLT was administered, both in total number and as a percent of 2W1S-specific T cells (**Figure 1c** and **d** and **Figure 2c** and **d** and **Supplementary Figure S2A** and **B**). It is known that $\alpha4\beta7^+$ cells migrate to the gut mucosa and intestine-draining mesenteric lymph nodes (MLNs).[20–22] This led us to speculate that the $\alpha4\beta7^+$ cells were migrating out of the CLN and into these mucosal tissues over time. To address this, we examined the MLN for the presence of 2W1S-specific, $\alpha4\beta7^+$ $CD4^+$ T cells. Although there was no difference at day 4, by day 9 a significantly greater proportion and total number of 2W1S-specific $CD4^+$ T cells were found in the MLN with dmLT immunization compared with CpG (**Figure 1** and **Supplementary Figure S2**); however, there was less difference between immunization groups in α4β7 expression on Ag-specific T cells in the MLN (**Figure 2**). This is

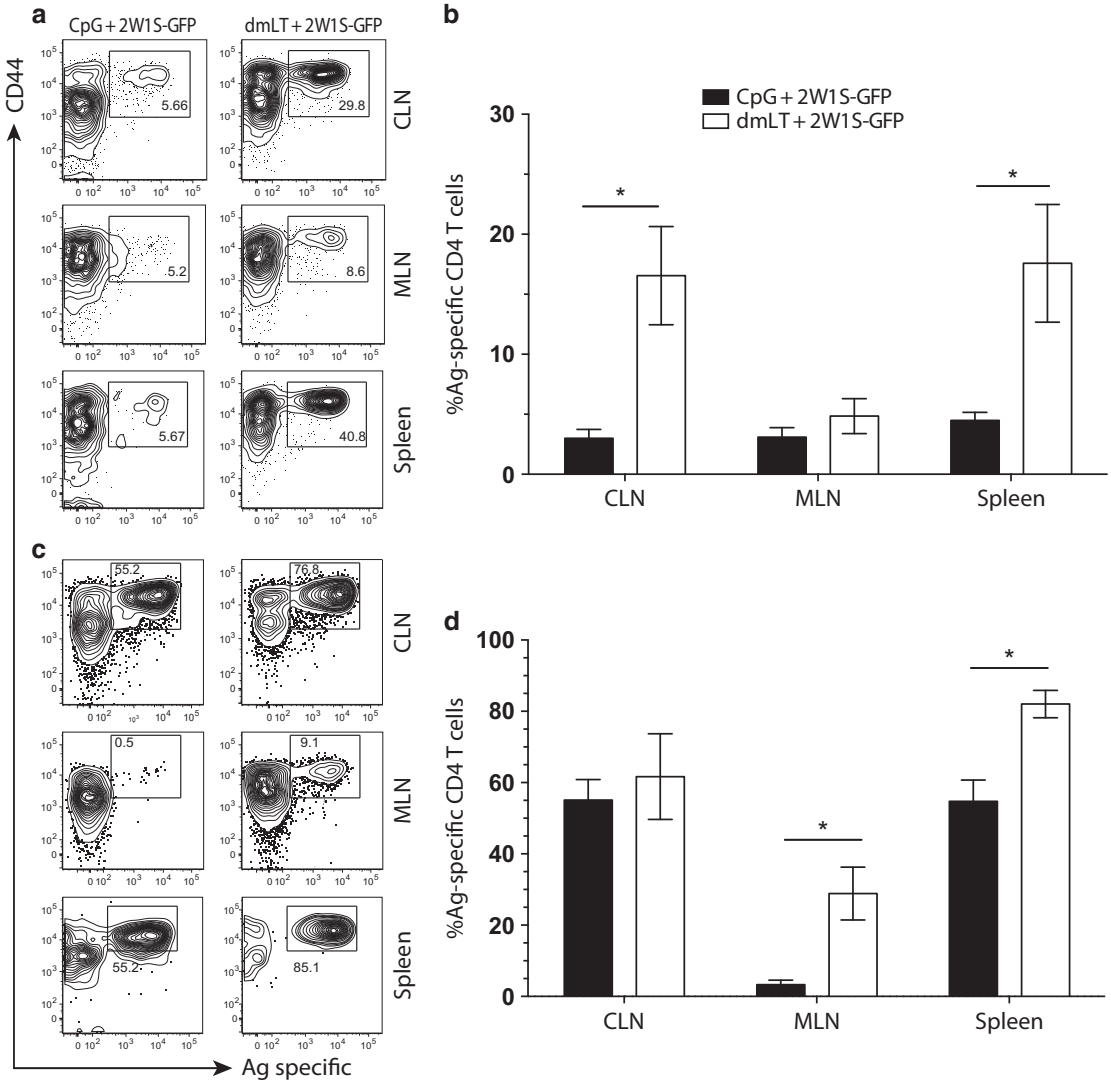

Figure 1 Both double-mutant heat-labile toxin (dmLT) and CpG induce potent, endogenous antigen-specific local and systemic CD4$^+$ T-cell responses following intradermal immunization. C57BL/6 mice were immunized intradermally in each ear pinna with CpG (left panes) or dmLT (right panes) plus 2W1S fused to green fluorescent protein (2W1S-GFP). Draining cervical lymph node (CLN), mesenteric lymph node (MLN), and spleens were collected at 4 days (**a** and **b**) or 9 days (**c** and **d**) post immunization. Collected tissues were dissociated and labeled with I-A^b:2W1S tetramer followed by magnetic bead enrichment of 2W1S-specific CD4$^+$ T cells. Enriched fractions were labeled with T-cell lineage-negative surface antibodies (CD19, CD11c, CD11b, and F4/80) along with CD4$^+$ T-cell markers (CD3, CD4$^+$, and CD44). Contour plots are representative of greater than six independent experiments with two to three mice per group. Numbers on each plot represent the percentage of cells in boxed gate. Graphs represent the pooled results of two experiments from more than six independent experiments with two to four mice per experiment. Significance was determined by student's two-tailed *t*-test with Holm–Sidak correction for multiple comparisons. Statistical significance is defined as follows: $^*P<0.05$, $^{**}P<0.01$, and $^{***}P<0.005$. Error bars represent s.e.m.

perhaps unsurprising and may be reflective of the fact that many cells entering the MLN should already express α4β7. Similar patterns were observed in the spleen, which functions as a surrogate of the systemic compartment (**Figures 1** and **2**). Interestingly, the gut-homing chemokine receptor CCR9 did not appear to be upregulated on 2W1S-specific CD4 T cells (data not shown). This shows that although both adjuvants can induce a potent, systemic antigen-specific CD4$^+$ T-cell response, dmLT was significantly better at upregulating α4β7 on antigen-specific endogenous CD4$^+$ T cells; however, it is clear that CpG also had the capacity to induce α4β7 to some degree.

As α4β7$^+$ lymphocytes are known to traffic to the intestinal mucosae,[21,23] we next assessed whether dmLT was specifically capable of routing antigen-specific CD4$^+$ T cells into the gut tissues following intradermal immunization. Mice were immunized intradermally with a single dose of dmLT or CpG plus 2W1S-GFP, and small and large intestines were assayed 9 and 14 days later for 2W1S-specific CD4$^+$ T-cell responses. We initially found there were little to no 2W1S-specific T cells detectable in the Peyer's patches or epithelial tissue (data not shown), so we focused on the intestinal lamina propria. On both days 9 and 14, 2W1S-specific CD4$^+$ T cells could be detected in the lamina propria of

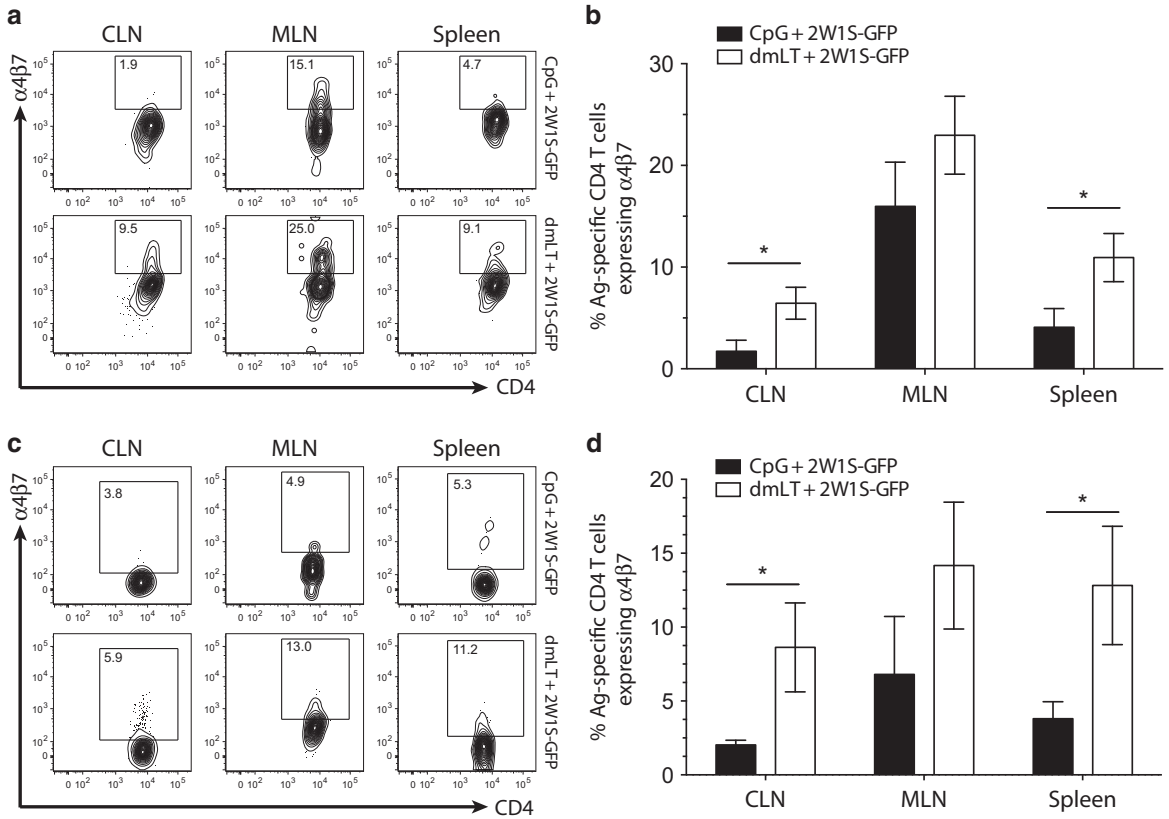

Figure 2 Intradermal immunization with double-mutant heat-labile toxin (dmLT) induces greater levels of α4β7 on 2W1S-specific CD4$^+$ T cells compared with CpG. Cell suspensions isolated from the cervical lymph node (CLN), mesenteric lymph node (MLN), and spleens of mice at day 4 (**a** and **b**) and day 9 (**c** and **d**) after intradermal immunization with either dmLT of CpG plus 2W1S fused to green fluorescent protein (2W1S-GFP) were surface stained with I-A^b:2W1S tetramer and enriched using magnetic beads then stained for CD4$^+$ T-cell markers and α4β7 expression. Contour plots shown are representative examples from six independent experiments with two to three mice per group. Numbers on each plot represent the percentage of cells in boxed gate. Top plots in (**a** and **c**) are representative of CpG$^+$ 2W1S-GFP immunized mice and the bottom plots represent dmLT$^+$ 2W1S-GFP from each tissue assayed. Graphs represent the pooled results of two experiments from more than six independent experiments with two to four mice per experiment. Significance was determined by student's two-tailed *t*-test with Holm–Sidak correction for multiple comparisons. Statistical significance is defined as follows: *$P<0.05$, **$P<0.01$, and ***$P<0.005$. Error bars represent s.e.m.

the small intestine (**Figure 3**) that were significantly higher in the dmLT immunized groups compared with CpG on day 9. There was also a substantial increase in 2W1S-specific CD4$^+$ T cells in the large intestine lamina propria at both time points that was reflected in the proportion and total number of 2W1S-specific T cells (**Figure 3** and **Supplementary Figure S2C**).

As we observed a greater overall response following dmLT immunization, it is possible this intestinal migration was simply a function of this increased number migrating into any non-lymphoid tissues and not actually a function of preferential movement. To address this possibility, we assessed lung responses to CpG vs. dmLT; at day 9 post-immunization there was no significant difference in the 2W1S-specfic CD4$^+$ T-cell responses (**Supplementary Figure S3**), supporting the hypothesis that dmLT induces specific migration to the intestinal mucosae. One other issue that arose is whether CpG is simply a poor adjuvant comparator for dmLT in terms of intestinal migration. To address this possibility, we substituted CpG with the Toll-like receptor-1/2 agonist, Pam3CSK(4). Similar to our data using CpG, Pam3CSK(4) had a limited capacity to induce α4β7 on antigen-specific T cells compared with dmLT (**Supplementary Figure S4**). Another possibility was that the immunization route itself was important for inducing a mucosal homing phenotype. As the tissue we chose to inject initially (the ear) drains to the same lymph node as the nasal-associated lymphoid tissue,[24] this may factor into the mucosal homing observation in dmLT immunization, particularly because nasal immunization is well-known to induce mucosal homing.[11,25,26] Modifying the route of administration could potentially eliminate the increased mucosal homing observed with dmLT immunization. We tested this by immunizing mice with dmLT by either intradermal immunization of the flank (where the associated lymph nodes do not also drain a mucosal tissue) or via more traditional intramuscular immunization. Notably, with either injection, α4β7 expression on 2W1S-specific T cells was comparable to intradermal ear immunizations (**Supplementary Figure S5**). These results suggest adjuvant choice, regardless of route, dictates T-cell intestinal migration characteristics, and that dmLT specifically drives this migration to a greater degree compared with other adjuvants.

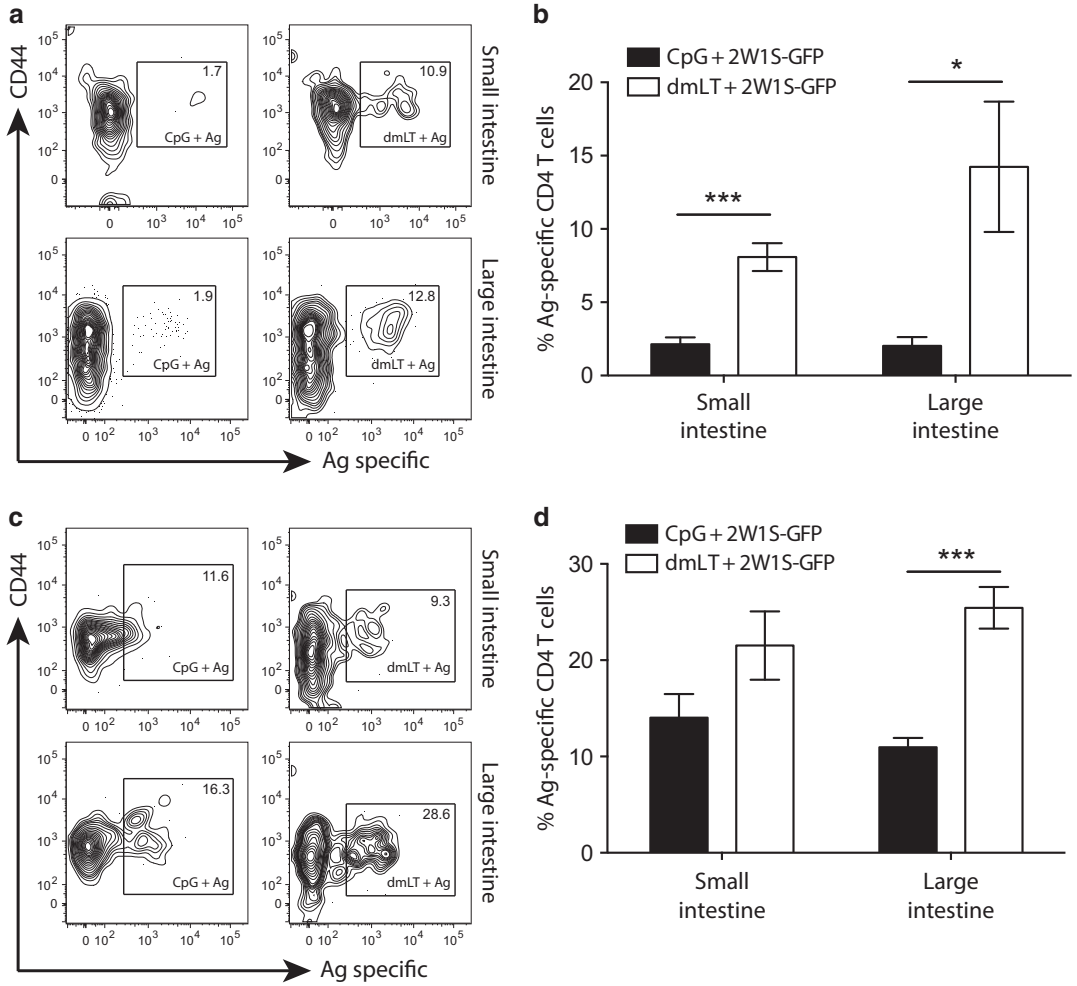

Figure 3 Antigen-specific T cells preferentially migrate into the small and large intestine lamina propria following intradermal double-mutant heat-labile toxin (dmLT) immunization. CpG or dmLT plus 2W1S fused to green fluorescent protein (2W1S-GFP) immunized mice were assayed at day 9 (**a** and **b**) or day 14 (**c** and **d**) for 2W1S-specific $CD4^+$ T-cell responses in the intestinal lamina propria. (**a** and **c**) Top contour plots are representative of the small intestine and the bottom plots are representative of the large intestine from three to four experiments for each tissue using two to three mice per experiment. Numbers on each plot represent the percentage of cells in boxed gate. (**b** and **d**) Graphs represent the pooled results of two experiments from four independent experiments with two to four mice per experiment. Significance was determined by student's two-tailed *t*-test with Holm–Sidak correction for multiple comparisons. Statistical significance is defined as follows: $^*P<0.05$, $^{**}P<0.01$, and $^{***}P<0.005$. Error bars represent s.e.m.

dmLT induces a balanced Th1/Th17 phenotype on antigen-specific $CD4^+$ T cells

In addition to the observation that dmLT can induce mucosal immune responses, it has also been shown that dmLT and related toxins are uniquely capable of driving balanced, or even "unpolarized" Th immune responses.[17,26–28] Although those studies characterized the phenotype imparted globally on bulk $CD4^+$ T cells or adoptively transferred monoclonal $CD4^+$ T cells, it is unknown how enterotoxins, such as dmLT, impact endogenous, antigen-specific $CD4^+$ phenotypes against companion antigens. To address this, mice were immunized intradermally in the ear with CpG or dmLT plus 2W1S-GFP and cytokine release from 2W1S-specific $CD4^+$ T cells was assessed following *in vitro* stimulation with 2W1S peptide. At 9 days post immunization, mice immunized with CpG predominantly made interferon-γ (IFN-γ) (**Figure 4a** and **b**), which was expected as CpG is known to polarize the Th1 phenotype in $CD4^+$ T cells.[29] Mice immunized with antigen plus dmLT also produced large amounts of IFN-γ; however, a portion of 2W1S-specific T cells also released significantly more IL-17A when compared with CpG (**Figure 4c** and **d**). These results suggest a balanced Th1/Th17 cytokine response when using dmLT as an adjuvant. Although the IFN-γ and IL-17 production was prominent, we also noted that Il-5 appeared to be produced at very low levels (data not shown). We also assessed whether the canonical Th1 and Th17 transcription factors (T-bet and Rorγt, respectively) were differentially expressed in dmLT vs. CpG immunized mice. We found that expression of these transcription factors tracked closely with the cytokine data (**Figure 5**). In addition, similar cytokine results were found in the spleen using an intravenous *in vivo* 2W1S peptide injection confirming that the results were not merely attributable to the effects of the *in vitro* stimulus (**Supplementary Figure S6**). This demonstrates that CpG

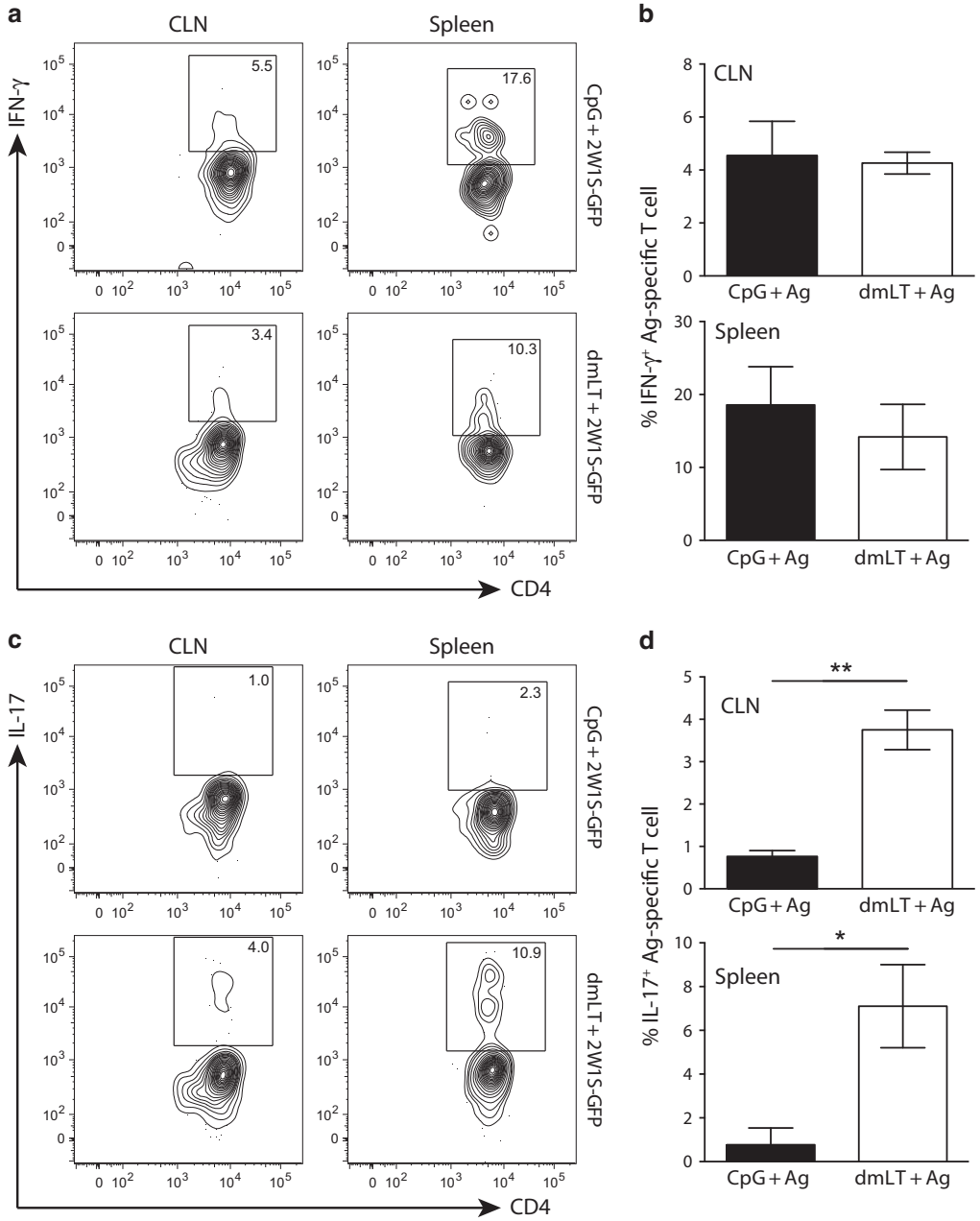

Figure 4 Double-mutant heat-labile toxin (dmLT) promotes a balanced Th1/Th17 cytokine phenotype in antigen-specific CD4$^+$ T cells following intradermal immunization. Mice were intradermally immunized with CpG or dmLT plus 2W1S fused to green fluorescent protein (2W1S-GFP) and the 2W1S-specific CD4$^+$ T-cell cytokine response was assessed on day nine. Cervical lymph node (CLN) and spleen were collected, dissociated, and plated into tissue culture dishes. Tissue explants were restimulated with 2W1S peptide for 6 h (the last four with Brefeldin A) then stained for CD4$^+$ T-cell markers and 2W1S specificity with tetramer followed by intracellular cytokine staining for interferon-γ (IFN-γ) (**a** and **b**) and interleukin (IL)-17A. (**c** and **d**). Contour plots are representative of cytokine staining from each immunization. Numbers on each plot represent the percentage of cells in boxed gate. Graphs represent one experiment with three to four mice per group and is representative of four independent experiments. Significance was determined by student's two-tailed *t*-test. Statistical significance is defined as follows: $^*P<0.05$, $^{**}P<0.01$, and $^{***}P<0.005$. Error bars represent s.e.m.

drives a dominant Th1 T cell response while dmLT appears to be capable of inducing a more balanced Th1/Th17 response in endogenous, antigen-specific CD4 T cells.

CD103$^+$ DCs present antigen and are required for dmLT-induced mucosal trafficking

To assess potential differences in each adjuvants' capacity to engage different populations of antigen presenting cells, we intradermally immunized mice with either dmLT or CpG plus 2W1S-GFP. One day later, when it is known that antigen has drained fully into lymph nodes,[30] CLNs were collected and single-cell preparations were stained with the newly described W6 antibody that preferentially detects 2W1S:I-A^b antigen-presenting complexes. This allowed us to quantify and phenotype cells specifically presenting the 2W1S peptide.[31] We selected markers to account for the major DC subsets

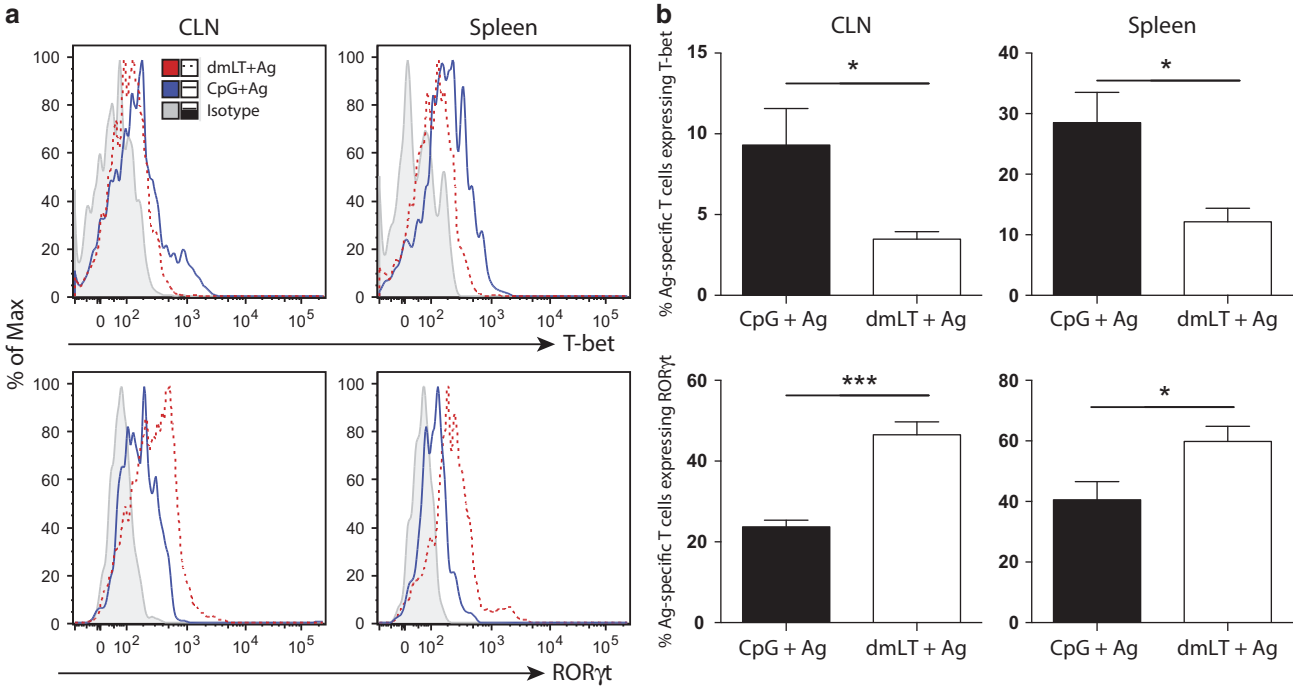

Figure 5 Double-mutant heat-labile toxin (dmLT) promotes a balanced Th1/Th17 transcriptional phenotype in antigen-specific CD4$^+$ T cells following intradermal immunization. Mice were intradermally immunized with CpG or dmLT plus 2W1S fused to green fluorescent protein (2W1S-GFP) and the 2W1S-specific CD4$^+$ T-cell transcription factor expression was assessed on day nine. Cervical lymph node (CLN) and spleen were collected, dissociated, and immediately stained for the intracellular transcription factors T-bet and Rorγt. (**a**) Representative histograms of each transcription factor are shown including the isotype control. (**b**) Graphs represent the percent of 2W1S-specific T cells expressing each transcription factor in immunized groups using five mice per group. Results are representative of four independent experiments. Significance was determined by student's two-tailed *t*-test. Statistical significance is defined as follows: *$P<0.05$, **$P<0.01$, and ***$P<0.005$. Error bars represent s.e.m.

located in the dermis: CD11c$^+$ CD11b$^+$; CD11c$^+$ CD11b$-$; CD11c$^+$ CD103$^+$, and Langerhans cells (EpCam$^+$ DEC-205$^+$).[32–34] **Figure 6a** shows CpG and dmLT both induced comparable overall levels of 2W1S peptide antigen presentation, which is quantified in **Figure 6b**; however, there were clear differences in the phenotype of cells presenting antigen in each immunization group. There was a fivefold greater proportion of CD11c$^+$ CD11b$-$ DCs presenting 2W1S antigen in response to dmLT compared with CpG (**Figure 6a** and **c**). Upon further examination of these CD11c$^+$ CD11b$-$ DCs, we found there were tenfold more CD103$^+$ dermal DCs presenting 2W1S in the dmLT immunized group. In fact, CD103$^+$ DCs accounted for roughly one-third of the CD11c$^+$ CD11b$-$ DCs in the dmLT immunized group. In addition, we observed that CpG plus 2W1S immunization induced more CD11b$^+$ CD11c$^+$ DCs to present 2W1S antigen in the CLN compared with dmLT. Lastly, we detected a slightly greater fraction of CD11b$^+$ CD11c$^+$ DEC-205$^+$ EpCam$^+$ DCs presented antigen in the dmLT immunization. It is likely to be these are Langerhans cells as they are the only DCs located in the epidermis known to express surface EpCam in conjunction with CD11c and DEC-205.[33]

It is known CD103 expression in a variety of tissue DCs correlates with intestinal homing.[10–12] Based on this and our data showing increased numbers of CD103$^+$ DCs presenting 2W1S antigen in the dmLT-immunized group, we hypothesized these DCs at least partly accounted for the higher expression of α4β7 and increased mucosal homing following immunization with dmLT. To test this, we immunized wild-type mice and mice deficient in the basic leucine zipper transcriptional factor ATF-like 3 (Batf3), which are unable to develop CD103-expressing DCs, including those found in the dermis (**Supplementary Figure S7** and ref. 35). Mice were immunized with dmLT plus 2W1S-GFP as before, and nine days post immunization, we analyzed 2W1S-specific T cells in the CLN, MLN, spleen, as well as the small and large intestine lamina propria. Local draining CLN and systemic splenic responses were equivalent, indicating there was no defect in the induction of 2W1S-specific T-cell responses (**Figure 7a**); however, there was a fivefold greater proportion of 2W1S-specific CD4$^+$ T cells in wild-type-immunized MLNs compared with Batf3$^{-/-}$ mice. Interestingly, the large intestine lamina propria was the only mucosal tissue affected by this deficiency (**Figure 7c**). In addition, α4β7 expression was significantly higher in the spleens of wild-type mice compared with Batf3$^{-/-}$ mice (**Figure 7b**). Notably, neither IL-17 nor IFN-γ production was affected in Batf3$^{-/-}$ mice, suggesting antigen presenting cells distinct from CD103$^+$ DCs might be inducing these cytokines (data not shown). These results imply CD103$^+$ dermal DCs preferentially present antigen in response to dmLT intradermal immunization. Although these cells are important for mucosal homing in response to dmLT

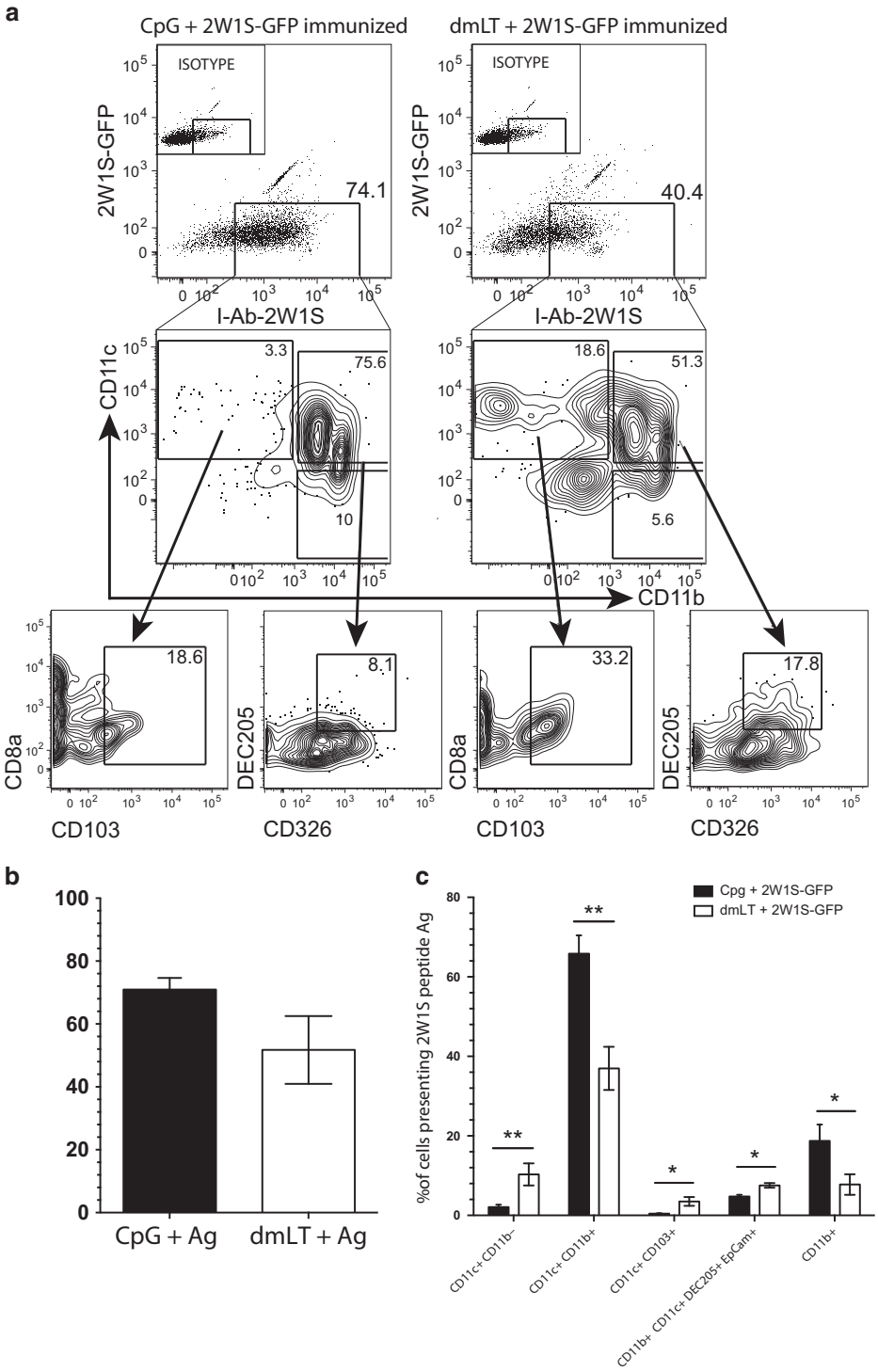

Figure 6 Intradermal immunization with double-mutant heat-labile toxin (dmLT) preferentially engages CD103$^+$ dermal dendritic cells and Langerhans cells compared with CpG. (**a**) C57BL/6 mice were immunized intradermally with either CpG (left panes) or dmLT (right panes) plus 2W1S fused to green fluorescent protein (2W1S-GFP). Twenty-four hours after immunization, draining cervical lymph node (CLN) were collected and dendritic cells (DCs) were isolated. Digested lymph nodes were labeled with anti-I:A^b:2W1S antibody and subjected to magnetic bead enrichment on cells presenting 2W1S. Cells were gated on B-cell lineage-negative and for dendritic cell/monocytes on CD11b and CD11c. Downstream gates show the level of expression of CD103 (on CD11c$^+$ CD11b $-$) or DEC-205 and CD326 (on CD11b$^+$ CD11c$^+$) or Langerhans cells. Numbers on each plot represent the percentage of cells in boxed gate. (**b**) Quantification of total antigen presentation of 2W1S antigen in each immunized group. From one independent experiment using three mice per group and representative of three independent experiments. (**c**) Graph represents differential antigen presentation by distinct DC subsets. Shown are two pooled independent experiments with three mice per group from a total of four independent experiments with two to four mice per group. Significance was determined by student's two-tailed *t*-test with Holm–Sidak correction for multiple comparisons. Statistical significance is defined as follows: $^*P<0.05$, $^{**}P<0.01$, and $^{***}P<0.005$. Error bars represent s.e.m.

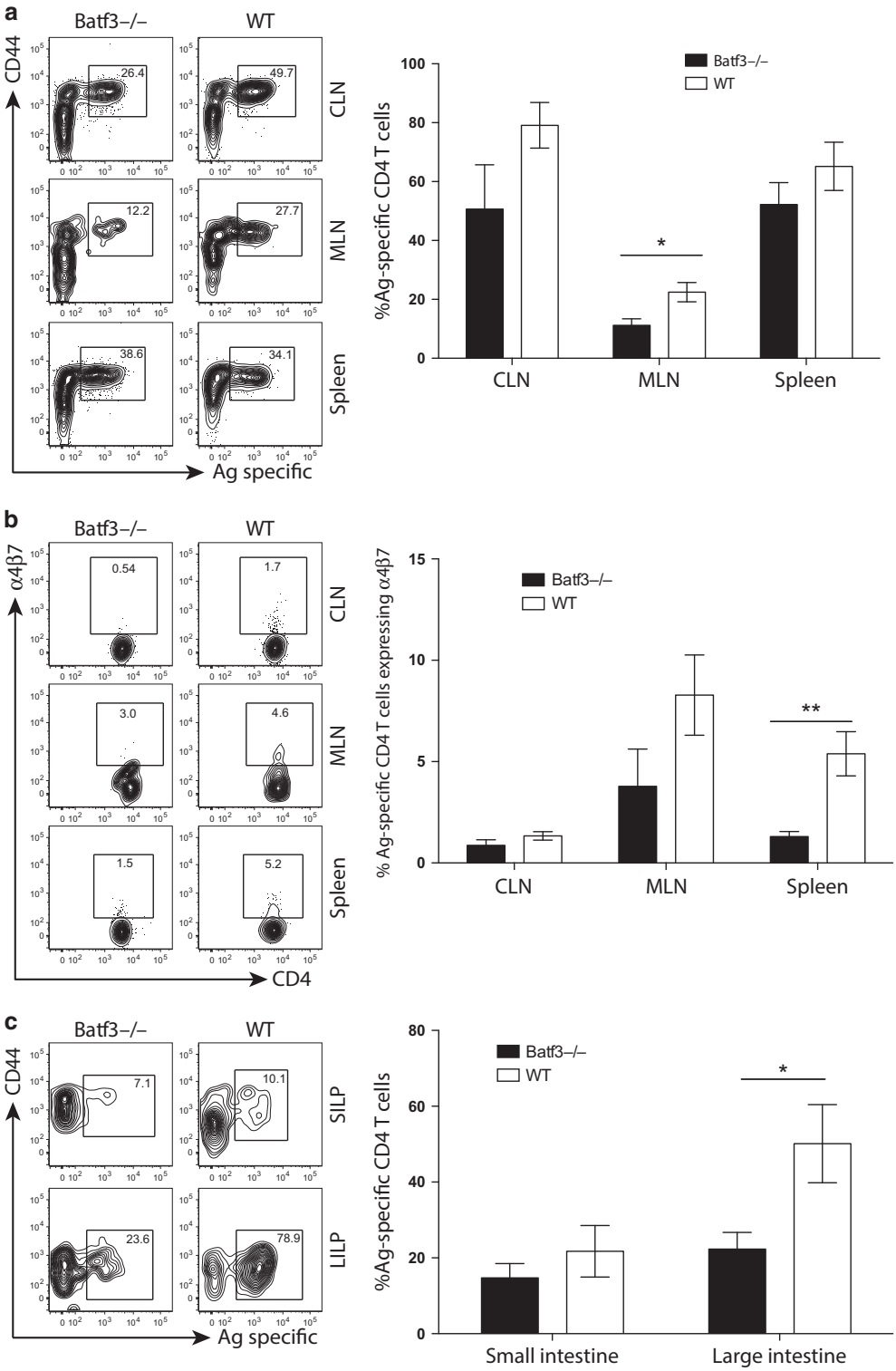

Figure 7 Batf3$^{-/-}$ mice have reduced mucosal phenotypes and homing in response to double-mutant heat-labile toxin (dmLT) immunization. Batf3$^{-/-}$ and wild-type (WT) mice were intradermally immunized with dmLT plus 2W1S fused to green fluorescent protein (2W1S-GFP). Nine days after immunization, cervical lymph node (CLN), mesenteric lymph node (MLN), spleen, and lamina propria were assayed for 2W1S-specific CD4$^+$ T cells and α4β7 expression using 2W1S:MHCII tetramers. Contour plots are representative of staining from each immunization. Numbers on each plot represent the percentage of cells in boxed gate. (**a**) Proportion of 2W1S-specific CD4$^+$4$^+$ CD4$^+$ T cells isolated from CLN, MLN ,and spleens. (**b**) Proportion of 2W1S-specific cells expressing α4β7 isolated from lymphoid tissue. (**c**) Proportion of 2W1S-specific CD4$^+$4$^+$ CD4$^+$ T cells isolated from small and large intestine. Data represent two pooled independent experiments from a total of three experiments with two to three mice per group. Significance was determined by student's two-tailed *t*-test with Holm–Sidak correction for multiple comparisons. Statistical significance is defined as follows: *$P<0.05$, **$P<0.01$, and ***$P<0.005$. Error bars represent s.e.m.

immunization, they do not appear to account for the presence of all 2W1S-specific T cells in the gut mucosae.

DISCUSSION

It is well accepted that adjuvants are essential mediators of vaccine induced immunity, yet it is not clear how, or even if, different adjuvants might be used to manipulate an immune response tailored to certain pathogen classes (i.e., enteric bacteria). Here we examined how adjuvant choice might determine the magnitude, homing, and phenotype of the endogenous, antigen-specific $CD4^+$ T-cell immune response with parenteral vaccination. Although Toll-like receptor agonists were excellent at inducing potent, antigen-specific $CD4^+$ T-cell responses, the type of response was one dimensional (predominantly Th1) and confined primarily to the local draining lymph nodes and spleen. In contrast, the bacterial enterotoxin-derived adjuvant dmLT induced a balanced cytokine response and stimulated robust migration of these cells to both the small and large intestinal mucosae. Induction of the gut homing integrin α4β7 was dependent on the presence of dermal $CD103^+$ DCs and mice lacking these cells were also deficient in inducing homing to the gut and gut-draining lymph nodes.

In this study, we administered immunizations parenterally, which is how most vaccines are currently delivered. This is the route of choice since it is technically easier, potentially less expensive, and not likely subject to the environmental enteropathy that affects orally administered vaccines. In addition, it circumvents potential side effects, such as Bell's Palsy or diarrhea, attributed to some mucosally delivered vaccines.[36,37] Although many of the findings presented here used intradermal injections, it was notable this route did not appear to be essential as intramuscular injections induced gut homing markers with equal efficiency. The implication of this result is that the adjuvant, not the route, is dictating the final phenotype and localization of the T-cell response.

These results confirm earlier observations that ADP-ribosylating toxins engage $CD103^+$ DCs after cutaneous administration;[38,39] however, this DC subset has never been previously demonstrated to affect $CD4^+$ T cells. This is the first direct evidence specifically demonstrating adjuvant choice guiding differential antigen presentation by distinctive DC subsets. This observation was achieved through the use of a recently described anti-peptide major histocompatibility complex class II antibody, which can precisely allow visualization of specific peptide:major histocompatibility complex class II complexes.[31] We also show epidermal Langerhans cells are preferentially engaged in the presence of dmLT compared with CpG. Combined, these are notable findings as it is likely this differential antigen presentation largely contributes to imparting a gut homing phenotype in addition to the diverse cytokine production seen in antigen-specific $CD4^+$ T cells from dmLT-immunized mice. Supporting this contention, the gut resident $CD103^+$ DC subset is known to impart α4β7 expression on $CD4^+$ T cells following intestinal antigen exposure.[10,12] Our evidence that $Batf3^{-/-}$ mice lacking CD103 DCs fail to induce the full expression of α4β7 and are deficient in large intestine homing supports the concept that $CD103^+$ skin DCs act similarly to those in the gut. With both adjuvants, there was a strong Th1 bias in 2W1S-specific $CD4^+$ T cells; however, dmLT also promoted a Th17 phenotype. It is notable $Batf3^{-/-}$ mice did not demonstrate significant defects in IL-17, implying other antigen presenting cells are possibly participating in priming Th17 cells in the presence of dmLT. The most likely candidate is Langerhans cells which were recently described as a prominent inducer of skin Th17 responses and in our experiments are also preferentially presenting 2W1S antigen in response to dmLT immunization compared with CpG.[40]

Although it is clear from this work $Batf3^{-/-}$ mice and the resulting CD103 DC deficiency are defective in targeting antigen-specific $CD4^+$ T cells to the large intestine, it appears these cells may be dispensable for migration to the small intestine. This is surprising considering expression of α4β7 is attenuated in the spleen and MLN in the absence of this DC subset. Although it has been shown T cells can migrate into the small intestine in the absence of α4β7,[41] it is also possible that this migration is more dependent on other homing molecules such as G-protein-coupled receptor 18 or CCR9, although in our hands, CCR9 was not significantly upregulated and may not contribute as much as other homing markers.[42,43] In addition, although our data shows a significant decrease in antigen-specific T-cell migration into the large intestine in $Batf3^{-/-}$ mice, this migration is not entirely abrogated, implying other DCs participate in the induction of mucosal homing. Langerhans cells, again, are possible candidates as they are a source of transforming growth factor-β1,[44] a cytokine important for inducing a mucosal homing phenotype.[45] In addition, other potential homing markers such as the recently described GPR15 may have a role in homing despite the downregulation of α4β7 in our study.[46,47] Notably, Hammerschmidt *et al.* showed that subcutaneously administered retinoic acid preferentially induced migration of antigen-specific T and B cells into the intestines.[48] In that study, retinoic acid also induced production of retinal dehydrogenase in skin-draining DCs, which could then impart a gut-homing phenotype on lymphocytes. It is possible that dmLT similarly affects DC function by inducing retinal dehydrogenase, leading to downstream T-cell migration into the gut. Future studies could potentially elucidate these mechanisms.

This work has important implications for vaccine design, particularly with respect to provoking specific immune responses tailored to certain pathogen classes. For example, it is known $CD4^+$ T cells are required for optimal immunity against the enteric pathogen *Salmonella*,[49] so supporting migration of *Salmonella*-specific $CD4^+$ T cells to the site of pathogen entry in the gut has the potential to prevent infection before the onset of severe pathology. It is possible this is true for other enteric pathogens such as *Shigella* or enterotoxigenic *E. coli*. One conclusion that can be drawn from this work is that adjuvant choice can have a significant impact on the outcome of vaccine-mediated immunity, both in terms of localization and cytokine phenotype of immune cells. It may be possible to use

these findings to explore the possibility of targeting other mucosal surfaces such as the respiratory or urogenital tract. Further, the possibility exists that combining adjuvants may have the potential to dramatically alter the type of immune response (humoral, Th1, Th17, and Th2), while retaining the capacity for migration to a relevant site. Alternatively, strict cytokine polarization observed in a particular formulation may impede the capacity to properly limit infection, and as such a balanced cytokine profile may be ideal in certain infections. Lastly, while it is well-appreciated adjuvants such as dmLT or cholera toxin can induce antigen-specific IgA responses at the intestinal mucosae,[7,17] it is not clear whether these adjuvants directly affect migration of vaccine-specific IgA-producing B cells to these sites. Our future studies will explore both possibilities and have the potential to shift the paradigm for how the next generation of vaccines are devised.

METHODS

Mice. C57BL/6 mice were purchased from Jackson Laboratories (Bar Harbor, ME) or from the NCI Mouse Repository via Charles River (Wilmington, MA). All mice used were female and ~8–12 weeks of age. Mice were housed under specific-pathogen-free conditions, and food and water were given *ad libitum*. BATF3$^{-/-}$ were purchased from Jackson Laboratories, bred in-house, and used for experimentation approximately at 8 weeks of age. The Tulane University Institutional Animal Care and Use Committee approved all procedures.

Fusion protein generation. Oligos were ordered (IDT, Coralville, IA) containing the 2W1S DNA sequence (peptide: EAWGALANWAVDSA) with *Bam*HI and *Eco*RI cut sites, 5′-GCGCTCTTTGGATCCGAGG CTTGGGGAGCATTGGCTAATTGGGCTGTGGACTCAGCTGAAT TCCCCTGTGAG-3′ (sense) and 5′-CTCACAGGGGAATTCAGCTGA GTCCACAGCCCAATTAGCCAATGCTCCCCAAGCCTCGGATC CAAAGAGCGC-3′ (antisense). Oligos were annealed and the resulting dimer was ligated into the pRSET-emeraldGFP cloning/expression vector (Life Technologies, Carlsbad, CA) using New BioLabs Quick Ligation Kit. The completed vector was then transformed into DH5α with ampicillin selection. Positive colonies were selected for plasmid isolation. Upon isolation of plasmid, the 2W1S-emGFP plasmid was transformed into Life Technologies BL21 Star (DE3) T7-expressing *E. coli* for protein expression. One liter of lag-phase cultures were induced with 1 mM isopropyl β-D-1-thiogalactopyranoside for 16 h and monitored for Emerald Green Fluorescent Protein expression. Protein was purified from bacterial lysates using the EMD Millipore (Temecula, CA) His-Bind Purification Kit. Before elution, the column was rinsed with 50 column volumes of 0.1% Triton X-114/phosphate-buffered saline at 4 °C to clear endotoxin. Eluted protein was then dialysed into phosphate-buffered saline and concentration was determined via spectrophotometry using extinction coefficient determined by ExPASy ProtParam tool (SIB Swiss Institute of Bioinformatics, Lausanne, Switzerland).

dmLT preparation. dmLT was obtained as previously described.[50] Briefly, purified dmLT was prepared from *E. coli* overnight cultures lysed in a micro fluidizer, dialysed, and fractionated by affinity chromatography on immobilized D-galactose columns. After elution, the protein was passed through an endotoxin removing resin resulting in purified adjuvant preparations with endotoxin levels less than 1 EU mg^{-1}.

Immunization and tissue processing. Mice were immunized in the dermis of the ear pinna in 7 µl of antigen containing 15 µg of 2W1S-emGFP fusion protein plus either 10 µg Invivogen Vaccigrade CpG ODN 2395 (San Diego, CA) or 2 µg of dmLT. Local T-cell responses were assayed by collecting both superficial CLN and distal responses were assayed by collecting the MLN and spleen. To isolate leukocytes, lymphoid tissue was mechanically dissociated and passed through a 100 µ m filter. Filtered cells were subsequently stained for flow cytometry and/or subjected to cell enrichment for antigen-specific T cells. I-A^b:2W1S-expressing S2 cells were grown in shaking 2 l flask with Schneider's drospholia medium supplemented with 10% serum and blasticidin to a density of 10^7 cell per ml. $CuSO_4$ and biotinylated monomers were purified using a EMD Millipore His-purification kit. Following elution, monomers were conjugated to allophycocyanin in a 1:4 (streptavidin-allophycocyanin:monomer) ratio. Antigen-specific cells were enriched as previously described.[14] Briefly, cells were incubated with 10 nM of I-A^b:2W1S tetramer for 1 h at room temperature in the presence of FcBlock. Samples were washed and incubated with Miltenyi (Bergisch Gladbach, Germany) anti-allophycocyanin microbeads for 20 min on ice. Resulting samples were washed, passed over Miltenyi LS columns and eluted cells were stained for further analysis.

Flow cytometry. Antibodies used for flow cytometry were as follows: Lineage negative cells were stained in vFluor450 including anti-CD11c (clone N418), anti-CD11b (clone M1/70), anti-F4/80 (clone BM8.1), and anti-CD19 (clone 6D5) purchased from Tonbo Biosciences (San Diego, CA). Anti-α4β7 PE (clone DAK32), anti-CD326 PE-Cy7 (clone G8.8), anti-CD4$^+$4 PE-Cy7 (clone IM7), anti-CD3ε FITC (clone 145-2C11), anti-CD19 PE-Dazzle (clone 6D5), anti-CD80 BV605 (clone 16-10A1), anti-CD86 BV605 (clone GL-1), anti-CD103 PerCP-Cy5.5 (clone 2E7), and streptavidin BV421 were purchased from BioLegend (San Diego, CA). Anti-I-A/I-E allophycocyanin (clone M5/114), DEC-205 PE (clone 205yekta), and anti-CD11b AF700 (clone M1/70) were purchased from eBioscience (San Diego, CA). For intracellular cytokine staining, anti-IFN-γ PerCP-Cy5.5 (clone XMG1.2), anti-IL-4 BV605 (clone 11B11), and anti-IL-17A PE-Cy7 (clone TC11-18H10.1) were purchased from BioLegend. Anti-IL-5 PE (clone TRK5) was purchased from eBioscience. GATA3 PE (clone L50-823) was purchased from BD Biosciences (San Diego, CA). For all surface staining protocols, cells were blocked with Fc Block mixed with 2% mouse and rat serum for 10 min on ice, then surface stained at 1:100 dilutions (DAK32 was used at 1:25 dilution; 2E7 at 1:50). Samples were collected using a BD Biosciences LSRII Fortessa cytometer. All fluorescence-activated cell sorting data was analyzed in FlowJo software v9.9.3 (FlowJo, LLC, Ashland, OR).

Intracellular staining. For restimulation, whole lymph node cell suspensions were stimulated with 25 µg 2W1S peptide in 1 ml volume for two hours in 37 °C, 5% CO_2. Without rinsing, 10 µg/ml of Brefeldin A was added to the media and allowed to continue incubating for four more hours (six total). Cells were washed and tetramer and surface stained as above. For intracellular staining, cells were permeabilized and fixed using BD Biosciences Perm/Fix intracellular staining kit and were stained rfo cytokines overnight. For transcription factor staining, cells were permeabilized using eBioscience FoxP3 staining buffer kit and stained overnight.

Anti-I-A^b:2W1S antibody purification and biotinylation. The monoclonal anti-I-A^b:2W1S antibody (called W6) was generated in-house as previously described.[31] Hybridoma cells were grown for 14 days and media was harvested and filtered. Cleared lystate was buffer exchanged to 50 mM sodium acetate (pH 5.0). Antibody was isolated using a ThermoFisher (Carlsbad, CA) Pierce Protein G chromatography column according to manufacturing specifications, with a flow rate of 1–3 ml min^{-1}. Bound antibody was stripped from the column using 0.1 M glycine, pH 2. Purified antibody was then exchanged into 0.1 M sodium bicarbonate buffer. Biotin-X-NHS mixture (2 mg ml^{-1}) prepared in dimethylsulfoxide was added to the antibody solution and incubated for 1 h in the dark at room temperature. After incubation, the solution was then exchanged into phosphate-buffered saline (pH 7.2) and filtered.

***In vivo* antigen presentation assay**. To assay the binding of the W6 antibody, C57BL/6 mice were immunized intradermally in the ear pinna with either Ovalbumin or 2W1S-GFP plus dmLT. CLNs were dissociated and the cell suspension was then digested with 300 M and l U ml^{-1} Collagenase D (Roche Applied Sciences) for 30 min at 37 °C. After digestion, the cell suspension was filtered and stained for 30 min on ice with the W6 antibody, washed and stained with streptavidin-phycoerythrin for 15 min on ice.

Statistics. All data sets collected or exported from FlowJo were analyzed in GraphPad Prism version 6 (GraphPad Software, La Jolla, CA). Statistical significance was determined using multiple *t*-tests with the Holm–Sidak correction for multiple tests or by individual *t*-tests. Significance was assigned as: $*P<0.05$, $**P<0.01$, and $***P<0.005$. Outliers were removed using the Grubb's outliers test. All graphs were generated in GraphPad Prism version 6.

SUPPLEMENTARY MATERIAL is linked to the online version of the paper at http://www.nature.com/mi

ACKNOWLEDGMENTS

We thank Dr Lisa Morici and members of the McLachlan Lab for critical reading of the manuscript. This work is supported by NIH grants R01 AI103343 and U01 AI124289 (to J.B.M.).

AUTHOR CONTRIBUTIONS

D.R.F., L.C.F., J.D.C. and J.B.M. designed research. D.R.F., J.A.G. and L.M.S. performed research. L.C.F. and J.D.C. contributed reagents. D.R.F., J.A.G. and J.B.M. analyzed data. D.R.F. and J.B.M. wrote the paper.

DISCLOSURE

The authors declare no conflict of interest.

REFERENCES

1. Global Burden of Disease Study 2013 Collaborators. Global Burden of Disease Study 2013 Collaborators Global, regional, and national incidence, prevalence, and years lived with disability for 301 acute and chronic diseases and injuries in 188 countries, 1990-2013: a systematic analysis for the Global Burden of Disease Study 2013. *Lancet* **386**, 743–800 (2015).
2. Grassly, N.C. *et al.* New strategies for the elimination of polio from India. *Science* **314**, 1150–1153 (2006).
3. World Health Organization Collaborative Study Group on Oral Poliovirus Vaccine. Factors affecting the immunogenicity of oral poliovirus vaccine: a prospective evaluation in Brazil and the Gambia. World Health Organization Collaborative Study Group on Oral Poliovirus Vaccine. *J. Infect. Dis.* **171**, 1097–1106 (1995).
4. Posey, D.L., Linkins, R.W., Oliveria, M.J., Monteiro, D. & Patriarca, P.A. The effect of diarrhea on oral poliovirus vaccine failure in Brazil. *J. Infect. Dis.* **175** (Suppl 1), S258–S263 (1997).
5. Heine, S.J. *et al.* Intradermal delivery of Shigella IpaB and IpaD type III secretion proteins: kinetics of cell recruitment and antigen uptake, mucosal and systemic immunity, and protection across serotypes. *J. Immunol.* **192**, 1630–1640 (2014).
6. Norton, E.B. *et al.* The novel adjuvant dmLT promotes dose sparing, mucosal immunity and longevity of antibody responses to the inactivated polio vaccine in a murine model. *Vaccine* **33**, 1909–1915 (2015).
7. Gloudemans, A.K. *et al.* The mucosal adjuvant cholera toxin B instructs non-mucosal dendritic cells to promote IgA production via retinoic acid and TGF-β. *PLoS ONE* **8**, e59822 (2013).
8. Yu, J. *et al.* Transcutaneous immunization using colonization factor and heat-labile enterotoxin induces correlates of protective immunity for enterotoxigenic *Escherichia coli*. *Infect. Immun.* **70**, 1056–1068 (2002).
9. Lavelle, E.C. *et al.* Effects of cholera toxin on innate and adaptive immunity and its application as an immunomodulatory agent. *J. Leukoc. Biol.* **75**, 756–763 (2004).
10. Welty, N.E. *et al.* Intestinal lamina propria dendritic cells maintain T cell homeostasis but do not affect commensalism. *J. Exp. Med.* **210**, 2011–2024 (2013).
11. Ruane, D. *et al.* Lung dendritic cells induce migration of protective T cells to the gastrointestinal tract. *J. Exp. Med.* **210**, 1871–1888 (2013).
12. Stock, A., Napolitani, G. & Cerundolo, V. Intestinal DC in migrational imprinting of immune cells. *Immunol. Cell Biol.* **91**, 240–249 (2013).
13. McLachlan, J.B., Catron, D.M., Moon, J.J. & Jenkins, M.K. Dendritic cell antigen presentation drives simultaneous cytokine production by effector and regulatory T cells in inflamed skin. *Immunity* **30**, 277–288 (2009).
14. Moon, J.J. *et al.* Naive CD4(+) T cell frequency varies for different epitopes and predicts repertoire diversity and response magnitude. *Immunity* **27**, 203–213 (2007).
15. Huseby, E.S. *et al.* How the T cell repertoire becomes peptide and MHC specific. *Cell* **122**, 247–260 (2005).
16. Rees, W. *et al.* An inverse relationship between T cell receptor affinity and antigen dose during CD4(+) T cell responses *in vivo* and *in vitro*. *Proc. Natl Acad. Sci. USA* **96**, 9781–9786 (1999).
17. Datta, S.K. *et al.* Mucosal adjuvant activity of cholera toxin requires Th17 cells and protects against inhalation anthrax. *Proc. Natl Acad. Sci. USA* **107**, 10638–10643 (2010).
18. Clements, J.D., Hartzog, N.M. & Lyon, F.L. Adjuvant activity of Escherichia coli heat-labile enterotoxin and effect on the induction of oral tolerance in mice to unrelated protein antigens. *Vaccine* **6**, 269–277 (1988).
19. Moon, J.J. *et al.* Tracking epitope-specific T cells. *Nat. Protoc.* **4**, 565–581 (2009).
20. Berlin, C. *et al.* α4β7 integrin mediates lymphocyte binding to the mucosal vascular addressin MAdCAM-1. *Cell* **74**, 185–195 (1993).
21. Petrovic, A. *et al.* LPAM (alpha 4 beta 7 integrin) is an important homing integrin on alloreactive T cells in the development of intestinal graft-versus-host disease. *Blood* **103**, 1542–1547 (2004).
22. Iwata, M. *et al.* Retinoic acid imprints gut-homing specificity on T cells. *Immunity* **21**, 527–538 (2004).
23. Berlin, C. *et al.* Alpha 4 beta 7 integrin mediates lymphocyte binding to the mucosal vascular addressin MAdCAM-1. *Cell* **74**, 185–195 (1993).
24. Wu, H.Y., Nikolova, E.B., Beagley, K.W., Eldridge, J.H. & Russell, M.W. Development of antibody-secreting cells and antigen-specific T cells in cervical lymph nodes after intranasal immunization. *Infect. Immun.* **65**, 227–235 (1997).
25. McNeal, M.M. *et al.* CD4 T cells are the only lymphocytes needed to protect mice against rotavirus shedding after intranasal immunization with a chimeric VP6 protein and the adjuvant LT(R192G). *J. Virol.* **76**, 560–568 (2002).
26. Mattsson, J. *et al.* Cholera toxin adjuvant promotes a balanced Th1/Th2/Th17 response independently of IL-12 and IL-17 by acting on Gsα in $CD11b^{+}$ DCs. *Mucosal Immunol.* **8**, 815–827 (2015).
27. Leach, S., Clements, J.D., Kaim, J. & Lundgren, A. The adjuvant double mutant Escherichia coli heat labile toxin enhances IL-17A production in human T cells specific for bacterial vaccine antigens. *PLoS ONE* **7**, e51718 (2012).
28. Meza-Sánchez, D., Pérez-Montesinos, G., Sánchez-García, J., Moreno, J. & Bonifaz, L.C. Intradermal immunization in the ear with cholera toxin and its non-toxic β subunit promotes efficient Th1 and Th17 differentiation dependent on migrating DCs. *Eur. J. Immunol.* **41**, 2894–2904 (2011).
29. Chu, R.S., Targoni, O.S., Krieg, A.M., Lehmann, P.V. & Harding, C.V. CpG oligodeoxynucleotides act as adjuvants that switch on T helper 1 (Th1) immunity. *J. Exp. Med.* **186**, 1623–1631 (1997).
30. Itano, A.A. *et al.* Distinct dendritic cell populations sequentially present antigen to CD4 T cells and stimulate different aspects of cell-mediated immunity. *Immunity* **19**, 47–57 (2003).
31. Spanier, J.A. *et al.* Efficient generation of monoclonal antibodies against peptide in the context of MHCII using magnetic enrichment. *Nat. Commun.* **7**, 11804 (2016).
32. Kaplan, D.H., Jenison, M.C., Saeland, S., Shlomchik, W.D. & Shlomchik, M.J. Epidermal langerhans cell-deficient mice develop enhanced contact hypersensitivity. *Immunity* **23**, 611–620 (2005).
33. Kaplan, D.H. *In vivo* function of Langerhans cells and dermal dendritic cells. *Trends Immunol.* **31**, 446–451 (2010).
34. Seré, K. *et al.* Two distinct types of Langerhans cells populate the skin during steady state and inflammation. *Immunity* **37**, 905–916 (2012).

35. Edelson, B.T. *et al.* Peripheral CD103+ dendritic cells form a unified subset developmentally related to CD8alpha+ conventional dendritic cells. *J. Exp. Med.* **207**, 823–836 (2010).
36. Lewis, D.J.M. *et al.* Transient facial nerve paralysis (Bell's palsy) following intranasal delivery of a genetically detoxified mutant of *Escherichia coli* heat labile toxin. *PLoS ONE* **4**, e6999 (2009).
37. Davitt, C.J.H. & Lavelle, E.C. Delivery strategies to enhance oral vaccination against enteric infections. *Adv. Drug Deliv. Rev.* **91**, 52–69 (2015).
38. Apte, S.H. *et al.* Subcutaneous cholera toxin exposure induces potent CD103(+) dermal dendritic cell activation and migration. *Eur. J. Immunol.* **43**, 2707–2717 (2013).
39. Olvera-Gomez, I. *et al.* Cholera toxin activates nonconventional adjuvant pathways that induce protective CD8 T-cell responses after epicutaneous vaccination. *Proc. Natl Acad. Sci. USA* **109**, 2072–2077 (2012).
40. Kashem, S.W. *et al.* Candida albicans morphology and dendritic cell subsets determine T helper cell differentiation. *Immunity* **42**, 356–366 (2015).
41. Kuklin, N.A. *et al.* alpha(4)beta(7) independent pathway for CD8(+) T cell-mediated intestinal immunity to rotavirus. *J. Clin. Invest.* **106**, 1541–1552 (2000).
42. Becker, A.M. *et al.* GPR18 controls reconstitution of mouse small intestine intraepithelial lymphocytes following bone marrow transplantation. *PLoS ONE* **10**, e0133854 (2015).
43. Stenstad, H. *et al.* Gut-associated lymphoid tissue-primed CD4+ T cells display CCR9-dependent and -independent homing to the small intestine. *Blood* **107**, 3447–3454 (2006).
44. Kaplan, D.H. *et al.* Autocrine/paracrine TGFβ1 is required for the development of epidermal Langerhans cells. *J. Exp. Med.* **204**, 2545–2552 (2007).
45. Kang, S.G., Park, J., Cho, J.Y., Ulrich, B. & Kim, C.H. Complementary roles of retinoic acid and TGF-β1 in coordinated expression of mucosal integrins by T cells. *Mucosal Immunol.* **4**, 66–82 (2010).
46. Kim, S.V. *et al.* GPR15-mediated homing controls immune homeostasis in the large intestine mucosa. *Science* **340**, 1456–1459 (2013).
47. Nguyen, L.P. *et al.* Role and species-specific expression of colon T cell homing receptor GPR15 in colitis. *Nat. Immunol.* **16**, 207–213 (2015).
48. Hammerschmidt, S.I. *et al.* Retinoic acid induces homing of protective T and B cells to the gut after subcutaneous immunization in mice. *J. Clin. Invest.* **121**, 3051–3061 (2011).
49. Johanns, T.M., Ertelt, J.M., Rowe, J.H. & Way, S.S. Regulatory T cell suppressive potency dictates the balance between bacterial proliferation and clearance during persistent *Salmonella* infection. *PLoS Pathog.* **6**, e1001043 (2010).
50. Norton, E.B., Lawson, L.B., Freytag, L.C. & Clements, J.D. Characterization of a mutant Escherichia coli heat-labile toxin, LT(R192G/L211A), as a safe and effective oral adjuvant. *Clin. Vaccine Immunol.* **18**, 546–551 (2011).